0026-895X/97/030473-09$3.00/0

MOLECULAR PHARMACOLOGY, **52:**473–481 (1997).

Nucleotide Regulation and Characteristics of Potassium Channel Opener Binding to Skeletal Muscle Membranes

K. E. J. DICKINSON, C. C. BRYSON, R. B. COHEN, L. ROGERS, D. W. GREEN, and K. S. ATWAL

Bristol-Myers Squibb Pharmaceutical Research Institute, Princeton, New Jersey 08543

Received September 11, 1996; Accepted May 14, 1997

SUMMARY

[^{3}H]P1075 binding to membrane preparations of rabbit skeletal muscle were observed in the presence of nucleotide triphosphates or diphosphates but not AMP, cAMP, adenosine, tripolyphosphate, or pyrophosphate. Nonhydrolyzable or poorly hydrolyzable ATP analogs inhibited MgATP-supported binding. The EC_{50} value for MgATP-supported binding (0.4 mM) was decreased ~10-fold in the presence of an ATP-regenerating system, and significant metabolism by membrane nucleotidases was confirmed by high performance liquid chromatographic analysis. [^{3}H]P1075 bound to skeletal muscle with a K_d value of 37 ± 3 nM and a B_{max} value of 280 ± 14 fmol/mg of protein. [^{3}H]P1075 binding to subcellular fractions was highest in membranes enriched in T tubules. Specific binding was reversible, trypsin-sensitive, maximal at pH 8, and stereoselective for the (3*S*,4*R*)-enantiomer of cromakalim. Potassium channel openers exhibited a rank order of potency of P1075 > pinacidil > levcromakalim = BMS-180448 > nicorandil > diazoxide = BRL 38226. Fluorescein analogs (ethyleosin, phloxine B, and rose bengal) were relatively potent inhibitors of binding (K_i = 200–300 nM). The potassium channel openers cromakalim and BMS-180448 were competitive inhibitors of [^{3}H]P1075 binding. In contrast, rose bengal and the ATP-regulated potassium channel antagonist glyburide increased the rate of [^{3}H]P1075 dissociation in a manner consistent with noncompetitive interaction.

$I_{K\text{-}ATP}$, which were first described in the heart, couple cellular metabolic status to the electrical excitability of the plasma membrane. Patch-clamp studies have also demonstrated their presence on pancreatic β, skeletal, smooth muscle, and brain cells (1). Antagonist and agonist drugs have been described that interact with these channels. Thus, the hypoglycemic sulfonylureas, such as glyburide, act as specific antagonists and inhibit $I_{K\text{-}ATP}$ opening induced by metabolic inhibition or KCOs. KCOs represent a structurally diverse class of compounds that open $I_{K\text{-}ATP}$ and thus have broad therapeutic potential. However, effective therapies for nonvascular indications are likely to require the introduction of tissue-selectivity because vasorelaxation and hypotension would produce unacceptable side effects. Indeed, cardioprotective KCOs structurally related to cromakalim have recently been described that have the cardioprotective potency of cromakalim but exhibit markedly diminished vascular activities (2). The KCO diazoxide also seems to be somewhat unique because it activates pancreatic β cell $I_{K\text{-}ATP}$ but functions, like tolbutamide, to inhibit cardiac channels (3). The basis for this tissue specificity is currently unknown but may relate to differences in $I_{K\text{-}ATP}$ isoforms.

Skeletal muscle contains a large abundance of $I_{K\text{-}ATP}$, which can be activated by KCOs such as levcromakalim (4) and pinacidil (5). Treatment with pinacidil mimicked the effects of ischemic preconditioning (6), which suggests that $I_{K\text{-}ATP}$ activation may be a protective mechanism during skeletal muscle anoxia. Treatment with the KCOs cromakalim and P1075 improved force recovery of rat skeletal muscle exposed to anoxia and reperfusion (7). Patch-clamp studies of mammalian skeletal muscle cells led to the development of models of $I_{K\text{-}ATP}$ that contain stimulatory and inhibitory nucleotide regulation sites (5, 8). Pinacidil is thought to open skeletal muscle $I_{K\text{-}ATP}$ by interaction with these sites (5). To examine the biochemical interaction of KCOs with skeletal muscle sites, we conducted binding studies using the potent KCO [^{3}H]P1075. Bray and Quast (9) and Quast *et al*. (10) used this radioligand to define a sulfonylurea-sensitive KCO binding site in endothelium-denuded rat aortic rings, which correlated with sites mediating vasorelaxation. The challenge of the current work was to define conditions that allowed KCO binding to skeletal muscle membranes because homogenization of cells or tissues results in loss of specific binding sites (9, 11). Thus, binding studies, to date, have necessitated the use of tissue rings (9, 10) or large numbers of viable cells (11).

$I_{K\text{-}ATP}$ are thought to consist of a complex of proteins, including ATP binding cassette protein or proteins (SUR) and inward rectifier protein or proteins (12). They are modulated by nucleotides (13) and phosphorylation states (14). In

ABBREVIATIONS: $I_{K\text{-}ATP}$, ATP-regulated potassium channel(s); SUR, sulfonylurea receptor; KCO, potassium channel opener; NDP, nucleotide diphosphate; SR, sarcoplasmic reticulum; AMP-PCP, β,γ-methylene-ATP; PKA, protein kinase A.

the current study, we examined the effects of these parameters on KCO binding and describe the pharmacological characteristics of a [^{3}H]P1075 binding site on rabbit skeletal muscle membranes.

Materials and Methods

Skeletal muscle membrane preparations. Rabbits (2.5–3 kg) were anesthetized with sodium pentobarbital, and their hindlimbs were dissected and weighed. Tissue was minced with scissors into 5 volumes (w/v) of 20 mM $NaHCO_3$ and 0.1 mM phenylmethylsulfonyl fluoride and homogenized using a Brinkmann Instruments Polytron homogenizer (4 × 10 sec, setting 7; Westbury, NY). The homogenate was centrifuged at 3,500 × *g* for 15 min at 4°, and the supernatant was filtered through cheesecloth. The filtrate was recentrifuged at 100,000 × *g* for 60 min, and the pellet was washed into 50 mM Tris·HCl, pH 7.4. The membranes were resuspended in 25 ml of 50 mM Tris·HCl, pH 7.4, at a protein concentration of 8–11 mg/ml and stored frozen in aliquots at −80°.

Skeletal muscle membranes were further purified for [^{3}H]P1075 localization studies as follows. Skeletal muscle (50 g) was homogenized for 1 min in 250 ml of 0.3 M sucrose and 5 mM imidazole, pH 7.4, in a Waring blender at maximum speed. The homogenate was centrifuged at 11,000 × *g* for 10 min, and the pellet was rehomogenized and recentrifuged. The supernatant was filtered through cheesecloth and centrifuged at 100,000 × *g* for 90 min. The pellet was resuspended in 0.3 M sucrose and 5 mM imidazole, pH 7.4, to a concentration of 3–5 mg/ml and layered onto a discontinuous sucrose gradient (27:32:38:45%) and centrifuged at 85,000 × *g* for 16–18 hr in an SW28 rotor. The membranes at the 10:25%, 27:32%, 32:38%, and 38:45% interfaces were designated A, B, C, and D, respectively. All membranes were collected, diluted 1:4 with 10 mM imidazole pH 7.4, and centrifuged 80,000 × *g* for 90 min. All pellets were rehomogenized in 0.3 M sucrose and 5 mM imidazole, pH 7.4, and stored at −80°.

A purified T tubule preparation was prepared as above except that the sucrose gradient consisted of 25:35:40:50%. The membranes at the 25:35, 35:40, and 40:50% interfaces were designated T tubules, light SR, and heavy SR, respectively. All membranes were collected, diluted 10-fold with 5 mM imidazole, pH 7.4, and centrifuged at 150,000 × *g* for 30 min. Light SR and heavy SR were rehomogenized in 0.3 M sucrose and 5 mM imidazole, pH 7.4, and stored at −80°. The pellet containing T tubules was homogenized in 0.3 M sucrose and 5 mM imidazole, pH 7.4, in a glass-Teflon homogenizer and then incubated (0.1 mg/ml) in a solution containing 50 mM potassium phosphate, pH 7.4, 3 mM $MgCl_2$, 0.15 M KCl, 0.3 mM $CaCl_2$, and 2 mM MgATP for 20 min at room temperature. This incubation allowed any contaminating SR to be loaded with phosphate and separated from T tubules in the subsequent density gradient. After the incubation, the protein was centrifuged at 150,000 × *g* for 30 min and resuspended in 2–3 ml of the loading solution. This solution was layered onto a second discontinuous sucrose gradient (35:50:63%) and centrifuged at 150,000 × *g* for 75 min in an SW28 rotor. The layer at the 10:35% interface was collected and diluted 10-fold with 5 mM imidazole, pH 7.4, and recentrifuged at 150,000 × *g* for 30 min. This final T tubule pellet was resuspended in 0.3 M sucrose and 5 mM imidazole, pH 7.4, and stored at −80°.

Enzyme marker assays. Analysis of Na^+/K^+-ATPase, Ca^{2+}/K^+-ATPase, and azide-sensitive-ATPase was performed according to Jones and Besch (15). Membranes used in the Na^+/K^+-ATPase assay were preincubated with 0.9 mg alamethicin/mg of membrane protein for 20 min at room temperature to unmask latent Na^+/K^+-ATPase activity. ATP blanks and phosphate standards were included to assess contaminating ATP in the reaction solutions and generate a standard curve.

The cholesterol content of membranes was determined using a cholesterol CII kit (Wako Biochemical Diagnostics, Edgewood, NJ). After hydrolysis of cholesterol esters, cholesterol was oxidized to produce hydrogen peroxide, which was measured colorimetrically.

[^{3}H]P1075 binding assay. Assays were conducted in 12 × 75-mm tubes in a total volume of 1 ml. The assay buffer consisted of 240 mM sucrose, 3 mM sodium orthovanadate, 2 mM $MgCl_2$, and 50 mM Tris·HCl, pH 7.4 The nucleotides (sodium or trilithium salts), [^{3}H]P1075 (14 nM, 51–61 Ci/mmol), and inhibitors were incubated with membranes (700 μg of rat brain, 50–200 μg of rabbit skeletal muscle, 500–700 μg of canine cardiac) for 60 (canine cardiac and rat brain) or 90 (skeletal muscle) min. Nonspecific binding was defined with 10 μM P1075. Bound and free radioligands were separated by filtration through a GF/C glass-fiber filter on a Brandel (Montreal, Quebec, Canada) cell harvester with three 2-ml washes of 50 mM Tris, pH 7.4, at 4°. The filters were transferred to 6-ml plastic scintillation vials, soaked overnight in 5 ml of scintillation fluid (Opti-fluor; Packard, Meriden, CT), and counted in a Packard liquid scintillation counter.

Nucleotide metabolism assay. Skeletal muscle membranes (7 mg/ml in 50 mM Tris/240 mM sucrose/4 mM $MgCl_2$) were incubated at 25° in 1 ml of buffer (50 mM Tris·HCl, pH 7.4, 240 mM sucrose, 4 mM $MgCl_2$, 2 mM ATP, 3 mM sodium orthovanadate) or an ATP regenerating system (1 mM dithiothreitol, 20 mM phosphocreatine, 10 units/ml creatine kinase, pH 7.4) or a system that removed enzymatically formed ATP (20 mM glucose, 15 units/ml hexokinase). The assay was initiated with the addition of membranes and stopped at appropriate times with the addition of 160 μl of 3 M $HClO_4$ to achieve a final acid concentration of 3%. Each sample was then placed in ice and homogenized at 4° for 10 sec and centrifuged at 3000 rpm for 20 min at 4°. The supernatant was removed and neutralized with 1 ml of 2 M $KHCO_3$. The neutralized samples were centrifuged at 3000 rpm for 20 min at 4°. The supernatants were removed, placed on ice, and filtered through a Millipore (Bedford, MA) 0.45-μm HV filter. Separation of the nucleotides was achieved by reversed-phase ion-pair chromatography on a Hewlett-Packard 1090 high performance liquid chromatograph equipped with a photodiode array detector and a Hewlett-Packard workstation computer interface. Samples (250 μl) were applied to a C_{18} 218TP54 (250 × 4.6 mm) 5-μm column equilibrated in 30 mM KH_2PO_4, pH 5, 5 mM tetrabutylammonium dihydrogen phosphate, and 4% CH_3CN (solvent A) at 1.5 ml/min. Nucleotides were eluted during a linear gradient of 0–35% solvent B (50% CH_3CN) over 35 min. The nucleotides were detected at 254 nm, and their elution times were identified using ATP, ADP, AMP, UTP, UDP, and UMP standards. Nucleotide peaks, calculated as the integrated area under the curve, were obtained as in milliabsorption units and converted to micromoles from comparison of standard curves. There was base-line-to-base-line separation of the nucleotides, and as little as 50 nmol was readily detected. The identity of the compounds in the peaks was also confirmed by mass spectrometry analysis. Analysis of ATP, ADP, UTP, and UDP incubated without membranes indicated there was no appreciable degradation of the compounds during the time course of the experiment.

Drugs. [^{3}H]P1075 was prepared in-house by catalytic tritiation of an olefinic precursor. Two tritium atoms were incorporated; the P1075 molecule and the resultant radioligand had a current specific activity of 51–61 Ci/mmol. The BMS compounds BMS-182264 [4-[[9-cyano-imino)[(1,2,2-trimethylpropyl)amino]methyl]amino]benzonitrile], BMS-180448 [3*S*-trans)-*N*-(4-chlorophenyl)-*N′*-cyano-*N″*-(6-cyano-3,4-dihydro-3-hydroxy-2,2-dimethyl-2*H*-1-benzopyran-4-yl)guanidine], and BMS-212345 [*cis*-1-(6-cyano-3,4-dihydro-3-hydroxy-2,2-dimethyl-2*H*-1-benzopyran-4-yl)-3-phenylurea] were also synthesized in-house.

Calculations. K_i values of competing drugs was calculated for IC_{50} values according to the equation of Cheng and Prusoff (16). Competition curves and saturation isotherms were analyzed to a four-parameter logistic equation using Sigma plot curve fitter, which fits data to nonlinear functions using the Marquardt-Levenberg algorithm. Goodness of fit to a one- or two-site binding model was determined by *F* test, in which $F = [SS_1 - SS_2)/(df_1 - df_2)]/SS_2/df_2$, where SS is the sum of squares of residuals with one- versus two-site

models and df is degrees of freedom of the corresponding models. Association rate constants (k_{+1}) were determined from pseudo-first-order plots using the equation $k_{+1} = k_{obs} - k_{-1}/L$, where k_{obs} is the observed association rate constant, and L is the radioligand concentration. Dissociation rate constants were calculated from the first-order plot of the dissociation reaction: $k_{-1} \cdot t = \ln[X/X_{eq}]$, where X is the specific radioligand bound at time t, and X_{eq} is the radioligand bound at equilibrium. The half-time values for dissociation reaction were calculated after linear regression analysis of this plot.

Results

Nucleotide regulation. Specific [^{3}H]P1075 binding (displaceable by 10 μM P1075) to rabbit skeletal muscle membranes was observed in the presence of sodium vanadate and MgATP. Vanadate alone was unable to support binding, and in the presence of vanadate and MgATP, binding was little different from binding with MgATP alone. These data suggest that MgATP was the key factor for supporting [^{3}H]P1075 binding. Membranes incubated with the catalytic subunit of PKA and MgATP had no greater binding than membranes incubated with MgATP alone (data not shown).

To explore the structural requirement for nucleotide regulation of [^{3}H]P1075 binding, a series of adenine nucleotide analogs were examined (all at 2 mM). Relative to MgATP (100%), ADP supported specific binding (75 ± 8%), whereas AMP (8 ± 2%), cAMP (9 ± 2%), and adenosine (1 ± 1%) were relatively inactive (Table 1). The phosphoryl component seemed less critical because pyrophosphate (4 ± 3%) and tripolyphosphate (3 ± 3%) were inactive. These data indicate the need for nucleotide triphosphates or diphosphates for [^{3}H]P1075 binding to be observed. The effects of different nucleotide triphosphates and diphosphates were further examined (Table 1). Most nucleotide triphosphates were able to support [^{3}H]P1075, and a number of the nucleotide triphosphates (GTP, ITP, UTP) were more effective than ATP for binding to rabbit skeletal muscle membranes. NDPs were generally less effective than their triphosphate counterparts, although UDP and IDP supported [^{3}H]P1075 binding membranes with similar efficacy to MgATP. Nonhydrolyzable triphosphates (AMP-PCP, β,γ-methylene-GTP, and α,β-methylene-ATP) were inactive, as was the nonhydrolyzable diphosphate (α,β-methylene-ADP). Although these agents could not support [^{3}H]P1075 binding *per se*, they were able to inhibit binding supported by MgATP. Thus, 5′-adenylylimido-diphosphate and AMP-PCP inhibited binding to skeletal muscle membranes with IC_{50} values of 2 and 7 mM, respectively.

TABLE 1

Relative abilities of nucleotides to support [^{3}H]P1075 binding to rabbit skeletal muscle membranes.

[^{3}H]P1075 binding was examined in the presence of the stated nucleotides (all at 2 mM) and included 2 mM $MgCl_2$ and 3 mM $NaVO_3$. Data are expressed as percent binding in the presence of ATP (100%) and represent mean ± standard error values of three experiments.

Nucleotide	Binding
	%
ATP	100 ± 0
GTP	134 ± 16
CTP	72 ± 12
dTTP	98 ± 16
ITP	139 ± 21
UTP	162 ± 11
ADP	75 ± 8
UDP	120 ± 16
GDP	69 ± 12
CDP	39 ± 13
IDP	93 ± 15
AMP	8 ± 2
cAMP	9 ± 2
Adenosine	1 ± 1
AMP-PCP	4 ± 1
α, β = Methylene-ATP	0 ± 0
α, β = Methylene-ADP	4 ± 2
β, γ = Methylene-GTP	7 ± 8

The concentration-response curve for the effects of MgATP on [^{3}H]P1075 binding to rabbit skeletal muscle membranes is shown in Fig. 1A. Under standard incubation conditions, the EC_{50} value of MgATP was 390 ± 23 μM (three experiments). The curve was steep, and the calculated Hill slope was 2.6 ± 0.07. This [^{3}H]P1075 binding could have resulted from metabolic products of added ATP because high performance liquid chromatographic analysis indicated a time-dependent loss of ATP with formation of AMP and ADP (Fig. 1B). The effect of an ATP-regenerating system was therefore examined. Regeneration of ATP preserved stable ATP levels with little formation of ADP or AMP (Fig. 1C). Under these conditions, a 10-fold leftward shift in the ATP dependency for [^{3}H]P1075 binding was observed (Fig. 1A), and the calculated EC_{50} value was 30 ± 9 μM with a slope factor of 1.7 ± 0.3. Maximal [^{3}H]P1075 binding was decreased by 80% in the presence of the regenerating system. This decrease was due to the presence of creatine phosphate, which inhibited ATP-supported binding in a dose-dependent manner (data not shown). These data suggest that MgATP was responsible for specific [^{3}H]P1075 binding but endogenous hydrolases underestimated its potency.

To examine whether [^{3}H]P1075 binding supported by ADP was due to metabolically produced ATP, binding was measured in the absence and presence of a system that reconverted ATP formed from ADP back to ADP (using glucose and hexokinase). In the presence of this hexokinase regeneration system, there was no formation of ATP, but AMP was formed by ADPase (data not shown). Under these conditions, maximal [^{3}H]P1075 binding was decreased by 70 ± 6%. Because the components of the hexokinase system had no effect on [^{3}H]P1075 binding, it was possible that as much as 70% of the ADP-supported binding resulted from ATP formed via transphosphorylation of added ADP.

Efforts to preserve NDP levels, by inhibiting ADPase, were unsuccessful because concentrations of inhibitors such as 5′-adenylylimido-diphosphate and trifluoperazine, which effectively inhibited ADPase activity, also decreased [^{3}H]P1075 binding (data not shown). Taken together, these data indicate that [^{3}H]P1075 binding was supported by nucleotide triphosphates and diphosphates. However, the quantitative contribution of certain NDPs was difficult to estimate because of transphosphorylation and ADPase reactions.

To examine the importance of phosphorylation for [^{3}H]P1075 binding, skeletal muscle membranes were treated with 100 units/ml calf alkaline phosphatase. This enzyme would be expected to dephosphorylate effector proteins. Binding supported by ATP or UTP was then measured. In the continued presence of alkaline phosphatase (during the binding reaction), [^{3}H]P1075 binding was eliminated by alkaline phosphatase treatment but unaffected by enzyme, which had been boiled. In contrast, membranes treated with enzyme

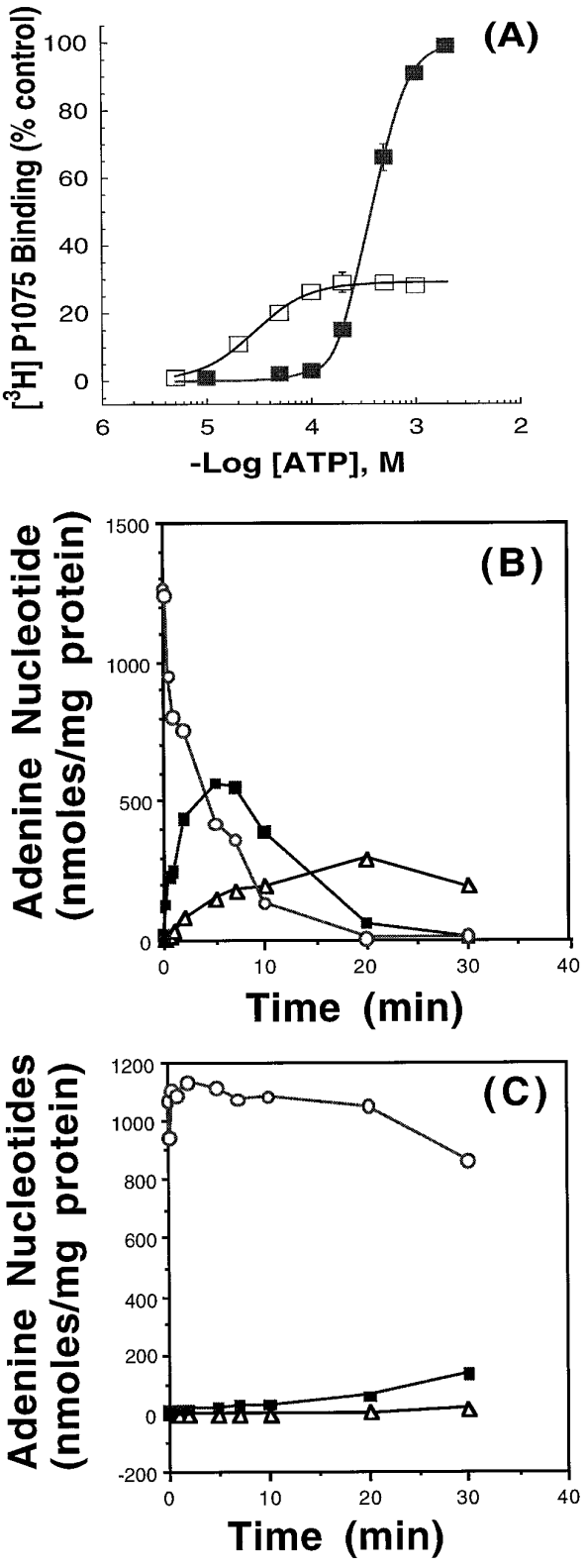

Fig. 1. Effect of an ATP regeneration system on [^{3}H]P1075 binding to rabbit skeletal muscle membranes and on adenine nucleotide levels. A, [^{3}H]P1075 binding to membranes was determined in the absence (■) or presence (□) of an ATP regeneration system (20 mM phosphocreatine, 10 units/ml creatine kinase). All samples contained 4 mM $MgCl_2$ and 1 mM dithiothreitol. Binding has been calculated as percent of control values in the absence of a regenerating system (mean = 63 ± 5 fmol/mg of protein at 14 nM [^{3}H]P1075). *Curves*, the computer-derived fits of mean data (± standard error) from three experiments using one-site analysis. B, Adenine nucleotide metabolism by skeletal muscle membranes. Membranes were incubated with 2 mM ATP for the stated times under standard binding assay conditions. Formation of ADP (■) and AMP (△) from added ATP (○) was determined using techniques described in Materials and Methods. C, Nucleotide metabolism was determined in the presence of an ATP-regeneration system, as described above.

and then washed retained [^{3}H]P1075 binding even in the presence of the general kinase inhibitor staurosporine. These data suggest that the phosphorylation state of the membranes regulated by endogenous kinases contributes to [^{3}H]P1075 binding.

Equilibrium, kinetics, and pH dependence. Specific [^{3}H]P1075 binding (14 nM) to rabbit skeletal muscle membranes at 25° reached equilibrium after 60 min. The association rate constant was 0.00110 ± 0.0004 nM/min (three experiments). Binding was reversible, and after the addition of excess P1075, the radioligand dissociated with a half-life of 16 ± 1.5 min (five experiments). The K_d value calculated as the ratio of the dissociation and association rate constants was 29 ± 4 nM (three experiments); this compared favorably with the K_d value calculated from saturation binding isotherms, which was 37 ± 3 nM (four experiments). The binding site maxima calculated from these experiments was 280 ± 14 fmol/mg of protein.

[^{3}H]P1075 binding was sensitive to proteolysis by trypsin. Thus, treatment of membranes with 30 μg/ml trypsin for 30 min at 37° resulted in 99% loss of [^{3}H]P1075 binding. Exposure of membranes to 10 mM *N*-ethylmaleimide for 10 min resulted in 80% loss of specific binding. Binding was maximal at pH 8–9 and decreased as the pH was lowered. At pH 6.2, specific binding was 25% of maximum binding.

Subcellular distribution. [^{3}H]P1075 binding to membrane fractions of rabbit skeletal muscle membranes was examined. Table 2 shows that binding was enriched in the P3 (100,000 × *g*) membrane fraction, which had high levels of plasma membrane (Na^+/K^+-ATPase) and SR (Ca^{2+}-ATPase) markers. [^{3}H]P1075 binding was not correlated with the activity of azide-sensitive ATPase or oligomycin-sensitive ATPase, a more specific mitochondrial marker (data not shown). Moreover, there was no enrichment of binding to a mitochondrial preparation of rabbit heart (data not shown). These data suggest that the membrane [^{3}H]P1075 binding sites were unlikely to be associated with mitochondria.

To examine the subcellular distribution in more detail, skeletal muscle membranes were fractionated to yield subcellular preparations enriched in specific organelles. Membranes that contained high activities of Ca^{2+}-ATPase (300–600 μmol/hr/mg of protein) had relatively low [^{3}H]P1075 binding (30–50 fmol/mg of protein), which suggests that high [^{3}H]P1075 binding of skeletal muscle was not due to its enrichment in SR. [^{3}H]P1075 binding was high (260 fmol/mg of protein) in membrane fraction A (see Materials and Methods), which had high levels of cholesterol, a marker for T tubules. Thus, a T tubule preparation was prepared that contained highly enriched [^{3}H]P1075 sites and a high cholesterol content (Table 2). This fraction was not enriched for Ca^{2+}-ATPase, Na^+/K^+-ATPase, or azide sensitive-ATPase. These data suggest that [^{3}H]P1075 binding sites were concentrated on T tubule-rich membranes.

Regional distribution. Specific [^{3}H]P1075 binding was also observed with guinea pig skeletal muscle, canine and rat

TABLE 2

Distribution of marker enzyme activities and [^{3}H]P1075 binding in subcellular membrane fractions of skeletal muscle.

Membrane fractions were prepared as described in Materials and Methods, and the stated enzyme activities and cholesterol levels were determined. [^{3}H]P1075 binding was determined using 14 nM. Values are mean ± standard error of two or three determinations.

Skeletal muscle membrane fraction	Specific [^{3}H]P1075 binding	Na^+/K^+-ATPase	Ca^{2+}-ATPase	Azide-sensitive ATPase	Cholesterol
	fmol/mg of protein		*μmol/hr/mg of protein*		
P1	44 ± 30	0	262	14.7	0.03
P2	38 ± 40	0.3	6.7	11.1	0.04
P3	160 ± 12	1.1	925	24.4	0.08
T tubules	309 ± 15	5.3	8.3	49	0.52

cardiac P2/P3 membrane preparations, and rat brain and liver. In contrast to rabbit skeletal muscle, vanadate increased binding to canine cardiac membranes in the presence of 2 mM MgATP by ~75%. Dissociation constants of [^{3}H]P1075 for canine cardiac (28 ± 5 nM) and rat brain (22 ± 15 nM) were similar to those of skeletal muscle, but B_{max} values were lower (73 ± 8 and 26 ± 10 fmol/mg of protein, respectively). Intermediate levels of [^{3}H]P1075 binding were observed in rat kidney, rabbit aorta, and sheep choroid plexus cells. Low or barely detectable levels were found in membranes from hamster insulinoma tumor and rat aortic smooth muscle cells and rat pancreas.

Competition by KCOs, antagonists, and fluoresceins. The specificity of the binding sites was examined by competition analyses. There was no significant inhibition of [^{3}H]P1075 binding by 100 μM concentration of verapamil, diltiazem, nifedipine, dofetilide, ryanodine, spermine, or spermidine or 10 mM tetraethylammonium. The amphipathic drugs propranolol and trifluoperazine (100 μM) inhibited [^{3}H]P1075 binding by only 31% and 48%, respectively.

The pharmacological characteristics of the binding sites were determined by competition experiments using KCOs from different chemical classes and $I_{K\text{-}ATP}$ antagonists. Table 3 shows the K_i values of drugs for [^{3}H]P1075 binding sites on rabbit skeletal muscle membranes. P1075 was the most potent inhibitor, and its calculated K_i value was similar to that determined from saturation analyses and kinetic determinations. Pinacidil was 7-fold weaker than P1075. BMS-182264 has a 4-cyanophenyl replacement for the pyridine ring of pinacidil; this chemical modification had little effect on potency for skeletal muscle [^{3}H]P1075 binding sites. The benzopyran KCO BMS-180448 was slightly more potent than levcromakalim. Binding sites demonstrated stereoselectivity because the (3*S*,4*R*)-enantiomer levcromakalim was 54-fold more potent than its (3*R*,4*S*)-enantiomer BRL 38226. BMS-212345, which is a benzopyran KCO with unfavorable cis stereochemistry, had markedly reduced binding potency, and its K_i value was similar to those of the weak KCOs nicorandil and diazoxide. In most cases, competition curves for KCOs had slope factors close to unity (Table 3). [^{3}H]P1075 binding sites on skeletal muscle membranes were similar to those on cardiac and brain membranes (data not shown). Thus, a correlation plot for nine KCOs from different chemical classes and the antagonist glyburide indicated a good agreement between these parameters (r^2 = 0.970 and 0.905, respectively).

The $I_{K\text{-}ATP}$ antagonists phentolamine and 5-hydroxydecanoate (or its lactone counterpart) were unable to inhibit [^{3}H]P1075 binding (Table 3). In contrast, the classic $I_{K\text{-}ATP}$ antagonist glyburide inhibited binding, and its calculated K_i value was 130 ± 20 nM. The slope factor of the glyburide inhibition curves was 0.77 ± 0.04 (three experiments; Table 3), which was significantly less than unity. Analysis of these data to a two-site binding model indicated putative high and low affinity components. High affinity glyburide sites had an apparent K_i value of 35 ± 21 nM, which represented 52 ± 24% of the specific binding sites. The low affinity sites had an apparent K_i value of 0.84 ± 0.47 μM.

Fluorescein and a number of its analogs inhibited [^{3}H]P1075 binding to rabbit skeletal muscle membranes in a concentration-dependent manner (Fig. 2). Competition curves exhibited Hill slopes that were close to unity (0.8–1.2). Table 4 shows the structures of the fluoresceins and the position of substituents using the numbering system derived from the lactone form of the molecule. Fluorescein was a weak inhibitor of [^{3}H]P1075 binding. Inhibitory potency was enhanced by the introduction of isothiocyanate in the 5-position of the phenyl ring. Further substitution with halogen atoms (in phloxine B and rose bengal) resulted in significantly enhanced potency (compare eosin Y and phloxine B). Eosins that contained bromo groups in positions 2′, 4′, 5′, and 7′ had increased potency compared with fluorescein derivatives, and ethyleosin exhibited a K_i value of 200 nM.

Kinetic studies of binding inhibition. We examined the effect of rose bengal on [^{3}H]P1075 dissociation from rabbit skeletal muscle membranes. After the attainment of equilibrium, the addition of excess P1075 dissociated [^{3}H]P1075 in a first-order reaction with a half-life of 14 ± 2 min (two experiments). Dissociation induced by rose bengal (10 μM) was markedly faster, and ~90% of binding dissociated at the earliest time point (1 min). These data suggest that the inhibition of [^{3}H]P1075 binding to membranes by fluoresceins was not competitive but was consistent with an allosteric or noncompetitive interaction.

The ability of BMS-180448 to dissociate [^{3}H]P1075 binding from rabbit skeletal muscle membranes was examined. Fig. 3 shows the dissociation of [^{3}H]P1075, expressed as first-order kinetics, that was initiated by a 50-fold excess (relative to K_i

TABLE 3

Inhibition constants of KCOs and $I_{K\text{-}ATP}$ antagonists for [^{3}H]P1075 binding sites on rabbit skeletal muscle membranes.

K_i values and slope factors (n_H) were calculated from competition curves as described in Materials and Methods. Values are mean ± standard error of three to seven determinations.

Compound	K_i	n_H
	μM	
KCO		
P1075	0.022 ± 0.002	0.89 ± 0.02
Pinacidil	0.16 ± 0.09	0.70 ± 0.13
BMS-182264	0.11 ± 0.02	0.91 ± 0.02
Levcromakalim	1.0 ± 0.2	0.95 ± 0.03
BRL 38226	54 ± 14	0.96 ± 0.07
BMS-180448	0.56 ± 0.05	0.80 ± 0.15
BMS-212345	22 ± 2	1.06 ± 0.01
Nicorandil	17 ± 3	0.95 ± 0.05
Diazoxide	62 ± 2	0.81 ± 0.02
Antagonist		
Glyburide	0.13 ± 0.02	0.77 ± 0.04
5-Hydroxy-decanoic acid	>100	
Phentolamine	>100	

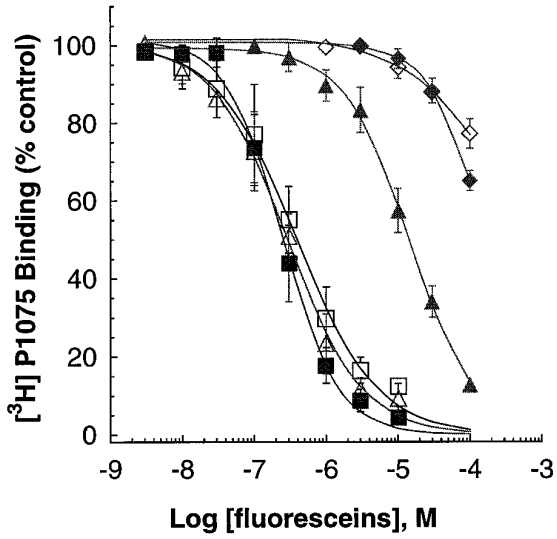

Fig. 2. Inhibition of [^{3}H]P1075 binding to rabbit skeletal muscle membranes by fluorescein derivatives. [^{3}H]P1075 (14 nM) was incubated with rose bengal (□), phloxine B (■), ethyl eosin (△), eosin maleimide (▲), fluorescein (◇), or dichlorofluorescein (◆) in the presence of MgATP (2 mM), and binding was assessed as described in Materials and Methods. Results are mean ± standard error values of three experiments.

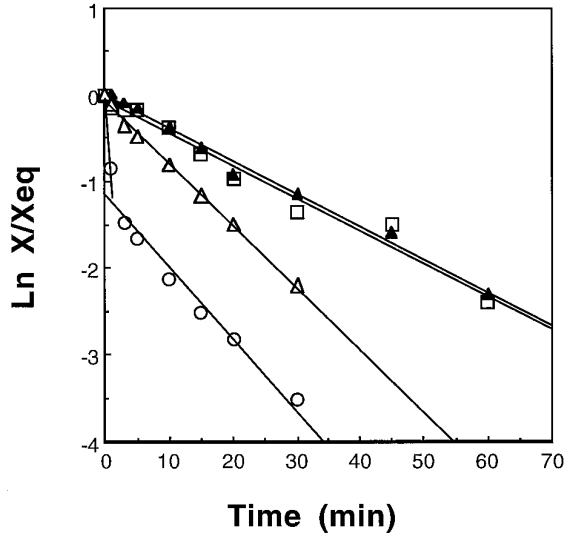

Fig. 3. Dissociation of [^{3}H]P1075 binding by KCOs and glyburide. [^{3}H]P1075 (15 nM) was incubated with rabbit skeletal muscle membranes until equilibrium was reached. Dissociation of [^{3}H]P1075 was initiated by P1075 (□, 1.35 μM), BMS-180448 (▲, 65 μM), or 10 μM P1075 and 0.1 (△) or 6.5 (○) μM glyburide, and binding was determined at the indicated times. Results are plotted as a first-order plot (see Materials and Methods). Results are representative of three experiments.

values) of P1075 or BMS-180448. This concentration of drug was calculated to occupy 98% of the primary binding sites. Dissociation rate constants determined using 50-fold excess P1075 (k_{-1} = 0.032 ± 0.007 min^{-1}) were similar to that obtained with saturating concentrations of drug (k_{-1} = 0.038 ± 0.006 min^{-1}). Dissociation induced by BMS-180448 was not different from these values (k_{-1} = 0.0330 ± 0.005 min^{-1}; three experiments), which suggests that P1075 and BMS-180448 competed for the same primary binding site. Kinetic experiments performed at 15 min after the addition of a 50-fold excess of competing drug suggested that levcromakalim and BMS-182264 were also competitive inhibitors of [^{3}H]P1075 binding.

TABLE 4

Potency of fluorescein analogs to inhibit [^{3}H]P1075 binding to rabbit skeletal muscle membranes.

Competition curves were obtained using 14 nM [^{3}H]P1075, and K_i values were calculated from the Cheng and Prusoff equation (16). Values are mean ± standard error of three experiments with different membrane preparations.

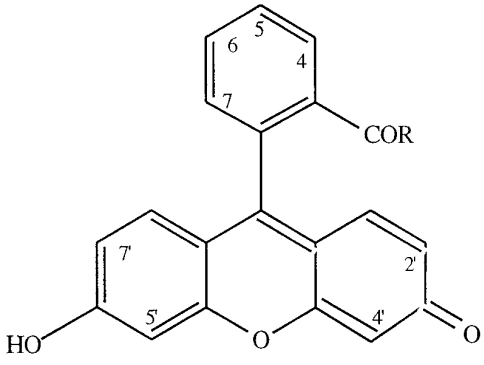

Compound	R^4	R^5	R^6	R^7	R	$R^{2'}$	$R^{4'}$	$R^{5'}$	$R^{7'}$	K_i
										μM
Fluorescein	H	H	H	H	OH	H	H	H	H	>100
Gallein	H	H	H	H	OH	H	OH	OH	H	64 ± 1.3
Dichlorofluorescein	H	H	H	H	OH	Cl	H	H	Cl	>100
Fluorescein isothiocyanate	H	NCS	H	H	OH	H	H	H	H	11 ± 4
Eosin Y	H	H	H	H	OH	Br	Br	Br	Br	6.5 ± 0.7
Ethyleosin	H	H	H	H	OC_2H_5	Br	Br	Br	Br	0.2 ± 0.07
Eosin isothiocyanate	H	NCS	H	H	OH	Br	Br	Br	Br	2.9 ± 1
Eosin maleimide	H	$N(CO)_2CC$	H	H	OH	Br	Br	Br	Br	8.7 ± 2
Eosin iodoacetamide	H	$NHCOCH_2I$	H	H	OH	Br	Br	Br	Br	2.4 ± 0.5
Phloxine B	Cl	Cl	Cl	Cl	OH	Br	Br	Br	Br	0.2 ± 0.05
Rose bengal	Cl	Cl	Cl	Cl	OH	I	I	I	I	0.3 ± 0.1

The mechanism of BMS-180448-mediated inhibition was also examined by performing [^{3}H]P1075 saturation isotherms. The mean K_d value for control membranes was 28 ± 4 nM, and in the presence of 1, 2, 3, and 5 μM BMS-180448, K_d values were 73 ± 16, 121, 170 ± 39, and 434 nM respectively (two to five experiments). The B_{max} value for control membranes (273 ± 12 fmol/mg of protein) was not significantly different from those in the presence of 1 μM (264 ± 32 fmol/mg of protein), 2 μM (258 fmol/mg of protein), 3 μM (278 ± 17 fmol/mg of protein), and 5 μM (311 fmol/mg of protein) BMS-180448, which confirms that BMS-180448 is a competitive inhibitor of [^{3}H]P1075 binding.

Glyburide was examined for its ability to dissociate [^{3}H]P1075 binding. Fig. 3 shows dissociation initiated by a combination of 10 μM P1075 and 0.1 μM glyburide ($t_{½}$ = 8.5 ± 1 min) was faster than that produced by P1075 alone. Dissociation appeared first order with this concentration of glyburide. However, the use of increased glyburide concentrations (≥2 μM) resulted in biphasic dissociation kinetics that did not model to a first-order reaction (Fig. 3). To define the EC_{50} value of glyburide for its interaction at the allosteric site or sites, dissociation was followed in response to glyburide in combination with 10 μM P1075. Glyburide (0.1–10 μM) increased [^{3}H]P1075 dissociation in a concentration-dependent manner. The EC_{50} value for this effect varied from 0.5 to 1.5 μM depending on the time point selected for the analysis (see Ref. 17). Because the dissociation reaction was not monophasic in the presence of high concentrations of glyburide, analysis of the EC_{50} value of glyburide through the use of apparent rate constants of dissociation (17) was not possible. However, it was clear on the basis of these experiments that glyburide exerted effects on [^{3}H]P1075 binding at concentrations of ≥0.1 μM.

Discussion

This study defined conditions that allowed [^{3}H]P1075 binding to be observed in membranes from skeletal muscle tissue. Previous [^{3}H]P1075 binding studies have used smooth muscle tissue (9, 10) but preliminary data indicate that viable cells may also be used (11). All studies to date report the loss of specific binding on homogenization of cells or tissue. The current work indicates that nucleotides are major regulators of KCO binding and their presence allows membrane [^{3}H]P1075 binding sites to be revealed. Initial studies showed that a "phosphorylation cocktail," containing PKA, vanadate, and MgATP, provided conditions that supported [^{3}H]P1075 binding to membranes. Further experiments established that PKA was unnecessary and the contribution of the phosphatase inhibitor sodium vanadate varied with the tissue source. These findings indicated that the key component for support of [^{3}H]P1075 binding to membranes was MgATP, and our previous inability to observe [^{3}H]P1075 binding to membranes may have resulted from rapid metabolism of added ATP by nucleotidases. Previous studies have also demonstrated the importance of MgATP for regulating the interaction of KCOs with SUR/$I_{K\text{-}ATP}$. Thus, inhibition of [^{3}H]glyburide binding by pinacidil was enhanced by ATP (18), and [^{3}H]P1075 binding to rat aortic rings was dependent on the metabolic status of the tissue, notably, the ATP levels (10).

When ATP metabolism was inhibited by a regenerating system, the EC_{50} value for support of [^{3}H]P1075 binding was 30 μM. This potency is similar to that for ATP-mediated inhibition of $I_{K\text{-}ATP}$ activity (1). However, in contrast to the ATP inhibitory site, which can also be occupied by nonhydrolyzable analogs of ATP, support of [^{3}H]P1075 binding required a hydrolyzable form of ATP. Moreover, the rank order of potency for nucleotide inhibition of $I_{K\text{-}ATP}$ [ATP ≫ ADP > AMP (13)] did not correlate with that for nucleotide interaction with the [^{3}H]P1075 sites. These data suggest that the nucleotide sites that supported [^{3}H]P1075 binding were unlikely to be the ATP inhibitory site of $I_{K\text{-}ATP}$. Nucleotide phosphates have been shown to inhibit [^{3}H]glyburide binding (18, 19) with a pharmacological profile that was similar to that for support of [^{3}H]P1075 binding. Thus, in the presence of Mg^{2+}, nucleotide triphosphates were equipotent to NDPs and monophosphates, and nonhydrolyzable forms of ATP and GTP were inactive (19). These findings suggest similarities in the nucleotide regulatory sites coupled to SUR and [^{3}H]P1075 binding.

[^{3}H]P1075 binding to membranes could have resulted from ATP-dependent phosphorylation and/or nucleotide binding to regulatory sites. Because the presence of alkaline phosphatase eliminated binding, it is likely that phosphorylation state is important. However, binding was supported by a broad range of nucleotide triphosphates, which contrasts with the high specificity of kinases for ATP. The ability of ATP to support binding seemed irreversible because added ATP was essentially degraded during the course of the incubation, and we noted no time-dependent decrease in binding. Our metabolism studies indicated marked interconversion of nucleotides during the course of the incubation. Thus, the marked degradation of ATP to ADP and AMP probably occurred via the action of an ADPase (20). Because we were unable to control this activity, the contribution of NDPs to [^{3}H]P1075 binding could not be accurately determined. Indeed, at least some portion of ADP-supported binding was likely due to its interconversion to ATP. In contrast, UDP was not transphosphorylated to a triphosphate but was degraded to an inactive monophosphate (data not shown). Therefore, it is likely that UDP supported [^{3}H]P1075 binding via its interaction with UDP/NDP recognition sites. Indeed, NDPs such as UDP have been shown to open Ca^{2+}-inactivated $I_{K\text{-}ATP}$ in skeletal muscle (4).

Fluorescein analogs have been shown to label active sites of Na^+/K^+-ATPase, perhaps by interaction with adenine recognition sites (21). They also modulate $I_{K\text{-}ATP}$ and SURs in brain and insulinoma cells (22, 23). Thus, fluoresceins such as rose bengal inhibited active $I_{K\text{-}ATP}$ and reactivated $I_{K\text{-}ATP}$ that had rundown (23), which suggests that they interact with activator and inhibitor nucleotide sites coupled to $I_{K\text{-}ATP}$. Fluoresceins also inhibited [^{3}H]glyburide binding to insulinoma and brain membranes, which suggests that their target sites are the SUR (22, 23). The basis for this inhibition seems to be an allosteric interaction because rose bengal increased the [^{3}H]glyburide dissociation rate (22). Based on these data, we were not surprised to discover that [^{3}H]P1075 binding to skeletal muscle membranes was inhibited by fluoresceins. Rose bengal and phloxine B were relatively potent inhibitors, with K_i values of 280 and 190 nM, respectively. Halogenated fluoresceins were generally more potent inhibitors of [^{3}H]P1075 binding, which correlated with their greater inhi-

bition of ^{86}Rb efflux in HIT cells (23). Inhibition of [^{3}H]P1075 binding by rose bengal also seems to involve an allosteric interaction. Thus, specific [^{3}H]P1075 binding to skeletal muscle membranes was dissociated by ~90% within 1 min. This rate of dissociation was significantly greater than that observed with excess P1075, which suggests that fluoresceins were potent allosteric or noncompetitive regulators of [^{3}H]P1075 binding.

In the presence of MgATP, the [^{3}H]P1075 binding sites exhibited characteristics of a drug/receptor interaction. Thus, binding was saturable, reversible, pH and trypsin sensitive, and highly specific for interaction with KCOs. The K_d value for [^{3}H]P1075 binding to membranes was ~30 nM, which was higher than the K_d values of 3–6 nM reported for binding to smooth muscle cells and tissue (9, 11). The [^{3}H]P1075 sites displayed many characteristics expected of a K_{ATP}-associated binding site, including stereoselectivity for the (3*S*,4*R*)-enantiomer of cromakalim and inhibition by the sulfonylurea glyburide. The KCO BMS-180448 has been shown to protect the myocardium in a glyburide-sensitive manner (2). In this study, we demonstrated that BMS-180448 increased the K_d value of [^{3}H]P1075 for skeletal muscle membranes without effects on the B_{max} value. These findings suggest that BMS-180448 competed directly for the [^{3}H]P1075 sites. In addition, BMS-180448, cromakalim, and BMS-182264 dissociated [^{3}H]P1075 from skeletal muscle membranes with similar rates to P1075, which suggests that these structurally diverse KCOs interacted directly, and competitively, with the labeled pyridinocyanoguanadinium recognition sites.

KCOs are generally assumed to target plasmalemmal $I_{K\text{-}ATP}$, although they have also been suggested to exert intracellular effects on Ca^{2+} regulation (for a review, see Ref. 24). These data imply there may be intracellular sites of action for P1075; however, examination of the subcellular distribution of [^{3}H]P1075 binding suggested little evidence of an intracellular location. Binding was enriched in P3 fractions and not associated with purified mitochondrial or SR preparations. In contrast, [^{3}H]P1075 binding was enriched in fractions high in cholesterol, which is a marker for T tubules. Therefore, it is likely that the observed skeletal muscle [^{3}H]P1075 sites are associated with T tubules. Skeletal muscle T tubules are in close proximity to the terminal cisternae of the SR and are involved in propagation of the action potential and Ca^{2+} release from the SR. These organelles also play a major role in the transport of ions into cells.

Glyburide has been reported to inhibit [^{3}H]P1075 binding to aortic smooth muscle, with an apparent K_i value of 400 nM, and significantly increase the [^{3}H]P1075 dissociation rates relative to that induced by P1075 (9). These data are consistent with allosteric interaction of glyburide with smooth muscle [^{3}H]P1075 sites. We obtained similar data with membrane preparations of skeletal muscle. Glyburide competed with [^{3}H]P1075 binding with an apparent K_i value of 130 nM. However, in contrast to the data of Bray and Quast (9), in which glyburide inhibition curves were steep, competition curves obtained with membranes had slopes less than unity, which could represent heterogeneous binding sites or negative heterotropic cooperative interactions. Dissociation experiments indicated that glyburide increased the [^{3}H]P1075 dissociation rate more significantly than the increase induced by excess P1075 and that high concentrations generated biphasic dissociation curves. The effect of glyburide to increase the dissociation rate of [^{3}H]P1075 occurred at relatively low glyburide concentrations (0.1–6 μM) in contrast to the high concentrations of glyburide required to produce such effects in rat aortic rings (9). These data support the concept that glyburide modulates KCO binding over physiologically relevant concentration ranges. Thus, patch-clamp studies have shown glyburide inhibited skeletal muscle $I_{K\text{-}ATP}$ with an apparent K_i value of 190 nM (8).

Acknowledgments

We thank for Bethanne Warrack, BMS (Analytical Chemistry), for mass spectrometric analysis of nucleotides and Dr. A. Hedberg for developing analytical models of binding data.

References

1. Lazdunski, M. ATP-sensitive potassium channels: an overview. *J. Cardiovasc. Pharmacol.* **24:**S1–S5 (1994).
2. Grover, G. J., J. R. McCullough, A. J. D'Alonzo, C. A. Sargent, and K. S. Atwal. Cardioprotective profile of the cardiac-selective ATP-sensitive channel opener BMS-180448. *J. Cardiovasc. Pharmacol.* **25:**40–50 (1995).
3. Faivre, J.-F., and I. Findley. Effects of tolbutamide, glibenclamide and diazoxide upon action potentials recorded from rat ventricular muscle. *Biochim. Biophys. Acta* **984:**1–5 (1989).
4. Hussain, M., and A. Wareham. Rundown and reactivation of ATP-sensitive potassium channels in mouse skeletal muscle. *J. Membr. Biol.* **141:**257–265 (1994).
5. Hehl, S., and B. Neumcke. Diverse effects of pinacidil on K_{ATP} channels in mouse skeletal muscle in the presence of different nucleotides. *Cardiovasc. Res.* **28:**841–846 (1994).
6. Jerome, S. N., T. Akimitsu, D. C. Gute, and R. J. Korthuis. Ischemic preconditioning attenuates capillary no-reflow by prolonged ischemia and reperfusion. *Am. J. Physiol.* **268:**H2063–H2067 (1995).
7. Weselcouch, E. O., C. Sargent, M. W. Wilde, and M. A. Smith. ATP-sensitive potassium channels and skeletal muscle function in vitro. *J. Pharmacol. Exp. Ther.* **267:**410–416 (1993).
8. Allard, B., and M. Lazdunski. Pharmacological properties of ATP-sensitive K^+ channels in mammalian skeletal muscle cells. *Eur. J. Pharmacol.* **236:**419–426 (1993).
9. Bray, K., and U. Quast. A specific binding site for K^+ channel openers in rat aorta. *J. Biol. Chem.* **267:**11689–11692 (1992).
10. Quast, U., K. M. Bray, H. Andres, P. W. Manley, Y. Baumlin, and J. Dosogne. Binding of the K^+ channel opener [^{3}H]P1075 in rat isolated aorta: relationship to functional effects of openers and blockers. *Mol. Pharmacol.* **43:**474–481 (1993).
11. Dickinson, K. E. J., R. B. Cohen, C. C. Bryson, D. E. Normandin, M. L. Conder, S. Gonzales S, J. R. McCullough, and K. S. Atwal. Characterization of K_{ATP} channels in smooth muscle cells and cardiac myocytes with [^{3}H]P1075 (abstract). *FASEB J.* **7:**A354 (1993).
12. Inagaki, N., T. Gonoi, J. P. Clement IV, N. Namba, J. Inazawa, G. Gonzalez, L. Aquilar-Bryan, S. Seino, and J. Bryan. Reconstitution of I_{KATP}: an inward rectifier subunit plus the sulfonylurea receptor. *Science (Washington D. C.)* **270:**1166–1170 (1995).
13. Terzic, A., R. Tung, and Y. Kurachi. Nucleotide regulation of ATP-sensitive potassium channels. *Cardiovasc. Res.* **28:**746–753 (1994).
14. Furukawa, T., V. Virag, N. Furukawa, T. Sawanobori, and M. Hiraoka. Mechanism for reactivation of the ATP-sensitive K^+ channel by MgATP complexes in guinea-pig ventricular myocytes. *J. Physiol.* **479:**95–107 (1994).
15. Jones, L. R., and H. R. Besch, Jr. Isolation of canine cardiac sarcolemmal vesicles. *Methods Pharmacol.* **5:**1–12 (1984).
16. Cheng, Y. C., and W. H. Prusoff. Relationship between the inhibition constant (K_i) and the concentration of the inhibitor which causes 50 per cent inhibition (I_{50}) of an enzymatic reaction. *Biochem. Pharmacol.* **22:** 3099–3109 (1973).
17. Kostenis, E., and K. Mohr. Two-point kinetic experiments to quantify allosteric effects on radioligand dissociation. *Trends Pharmacol. Sci.* **17:** 280–283 (1996).
18. Schwanstecher, M, C. Brandt, S. Behrends, U. Schaupp, and U. Panten U. Effect of MgATP on pinacidil-induced displacement of glibenclamide from the sulfonylurea receptor in a pancreatic β-cell line and rat cerebral cortex. *Br. J. Pharmacol.* **106:**295–301 (1992).
19. Gopalakrishnan, M., D. E. Johnson, R. A. Janis, and D. J. Triggle. Characterization of binding of the ATP-sensitive potassium channel ligand, [^{3}H]glyburide, to neuronal and muscle preparations. *J. Pharmacol. Exp. Ther.* **257:**1162–1171 (1991).
20. P. Meghji, J. D. Pearson, and L. L. Slakey. Regulation of extracellular adenosine production by ectonucleotidases of adult rat ventricular myocytes. *Am. J. Physiol.* **263:**H40–H47 (1992).
21. Farley, R. A., C. M. Tran, C. T. Carilli, D. Hawke, and J. E. Shively. The

amino acid sequence of a fluorescein-labeled peptide from the active site of (Na,K)-ATPase. *J. Biol. Chem.* **259:**9532–9535 (1984).
22. Holemans, S., O. Feron, J. Octave, and J. Maloteaux. Interaction of fluorescein derivatives with glibenclamide binding sites in rat brain. *Neurosci. Lett.* **183:**183–186 (1995).
23. De Weille, J., M. Muller, and M. Lazdunski. Activation and inhibition of ATP-sensitive K^+ channels by fluorescein derivatives. *J. Biol. Chem.* **267:** 4557–4563 (1992).
24. Quast, U. Do the K^+ channel openers relax smooth muscle by opening K^+ channels? *Trends. Pharmacol. Sci.* **14:**332–337 (1993).

Send reprint requests to: Dr. K. E. J. Dickinson, Senior Research Investigator, Department Cardiovascular Pharmacology, Bristol-Myers Squibb P.R.I., P.O. Box 4000, Princeton, NJ 08543-4000. E-mail: dickinson_kenneth_e.prilvms3@msmail.bms.com